

Engineering Notes

ENGINEERING NOTES are short manuscripts describing new developments or important results of a preliminary nature. These Notes should not exceed 2500 words (where a figure or table counts as 200 words). Following informal review by the Editors, they may be published within a few months of the date of receipt. Style requirements are the same as for regular contributions (see inside back cover).

Numerical Continuation of Torque-Free Motions of Gyrostats

Giulio Avanzini*

Politecnico di Torino, 10129 Turin, Italy

and

Guido de Matteis† and Paolo Petritoli‡

University of Rome “La Sapienza,” 00184 Rome, Italy

I. Introduction

IN this Note, the use of a numerical continuation method^{1,2} for tracing branches of periodic solutions of systems of ordinary differential equations that describe the motion of a dual-spin spacecraft with an unbalanced rotor, is presented. From the studies in Refs. 3 and 4, where the problem of continuation of periodic solutions for Hamiltonian systems was addressed, the novel approach proposed here deals with the Jacobian matrix singularity induced by conservation of a vector quantity. The parameter space is efficiently spanned to determine periodic solutions in the time domain and characterize their stability.

Gyrostat dynamics can exhibit a complex behavior that deserves attention, particularly in the presence of rotor unbalance and/or when the satellite is equipped with dampers, the axis of which is not precisely oriented along one of the principal axes. Among many papers on the subject, we recall the study by Hall,⁵ in which the despin maneuver of a simple gyrostat is analyzed as a sequence of quasi steady states and, more recently, the determination of equilibria of a gyrostat with axial damper carried out by Sandfry and Hall.^{6,7} In those papers, in which several references to the problem of gyrostat dynamics can be found, branches of stationary solutions were traced by a numerical continuation method as one of the gyrostat parameters was varied.

The simple gyrostat, the state vector of which is constrained on a sphere \mathcal{S} , is used as a test benchmark for the method (case 1). This first result can be seen as a complement to Ref. 5 because the complete phase portrait of the system is determined with a limited number of continuation segments for several values of the angular momentum stored in the rotor. Complex dynamic behavior that cannot be investigated by classic analytical tools is considered in case 2, when a viscous damper and an unbalanced rotor are introduced

into the system, the latter acting as a forcing term that perturbs the system so that steady spin equilibria no longer exist.

II. Continuation of Periodic Solutions for Conservative Systems

The capability of numerical continuation methods to trace branches of equilibria and periodic solutions is well known.^{1,2} Consider a system where $I(\mathbf{x}) = \text{const}$, when $\mathbf{x}(t)$ is a solution of the equation $\dot{\mathbf{x}} = \mathbf{f}(\mathbf{x}, \boldsymbol{\lambda})$, that is, when I is a first integral of the vector field \mathbf{f} . As stated in the cylinder theorem,⁸ a whole family of periodic solutions parametrized with respect to I exists, provided that a closed orbit $\mathbf{x}(t)$ is determined. As a consequence, a periodic solution of a conservative system is never isolated in the phase space, and continuation cannot be applied.

The problem is solved in Ref. 3 by exploiting the capability of the pseudo-arc length continuation of following vertical branches in the augmented phase space $\mathbb{R} \times \mathbb{R}^n$. Periodic solutions of the perturbed system

$$\dot{\mathbf{x}} = \mathbf{f}(\mathbf{x}, \boldsymbol{\lambda}) + \mu \nabla I \quad (1)$$

disappear when $\mu \neq 0$, with the additional term $\mu \nabla I$ acting like damping when $\mu < 0$. If a continuation is started from an equilibrium solution where $\mathbf{f} = 0$, the system undergoes a Hopf bifurcation when the unfolding parameter μ used as the continuation variable vanishes, as described in Ref. 3. It is then possible to start a continuation from the Hopf bifurcation that will determine a branch of periodic solutions for $\mu = 0$, that is, the orbits of the nominal system. Here this approach is called explicit unfolding, inasmuch as the nominal behavior of the system is recovered by an explicit continuation with respect to μ , as briefly outlined earlier. Application of the continuation method to a conservative system was demonstrated in recent times⁴ for the study of periodic orbits around Lagrange points, where the total energy is the only first integral of the system.

Consider now the dynamics of a mechanical system described by a set of ordinary differential equations (ODE), where the state vector \mathbf{x} is made of, or contains, the components of a vector quantity \mathbf{y} that is conserved, that is, $\mathbf{x}^T = [\mathbf{y}^T, \mathbf{z}^T]$. Because the modulus of \mathbf{y} is a first integral, the value of $M(\mathbf{y}) = \mathbf{y}^T \mathbf{y}$ can be used to parametrize the hypersurfaces $\mathcal{S} \subset \mathbb{R}^n$, such that $\mathbf{y}(t) \in \mathcal{S}$ when $\mathbf{x}(t)$ is a solution of the considered set of ODEs. Scaling the set of ODEs with respect to \mathbf{y} , we have $M(\mathbf{y}) = 1$ in the nominal case, and the relative manifold is the unit sphere S_0 . At this point, it is possible to unfold the branch of periodic orbits on S_0 if there exists a perturbation of the vector field \mathbf{f} that drives the solution $\mathbf{x}(t)$ toward S_0 . To this end, the elements $\dot{\mathbf{y}} = \mathbf{f}_y$ of the vector field \mathbf{f} are modified as follows

$$\dot{\mathbf{y}} = \mathbf{f}_y(\mathbf{x}, \boldsymbol{\lambda}) + \nu[1 - M(\mathbf{y})]\mathbf{y} \quad (2)$$

so that, when the parameter ν is properly assigned, S_0 is turned into a globally attractive manifold; that is, $\mathbf{x}(t)$ converges onto the hypersurface S_0 for $t \rightarrow \infty$. The nominal behavior of the dynamic system is asymptotically recovered for arbitrary initial conditions, and singular periodic solutions on S_0 are transformed into limit cycles for Eq. (2).

Because the phase portrait of the nominal system is implicitly contained in that of the augmented system, the methodology just discussed will be referred to as implicit unfolding. The unfolding parameter ν never vanishes, and its value governs the rate at which the

Presented as Paper 2004-5206 at the AIAA/AAS Astrodynamics Specialist Conference, Providence, RI, 16–19 August 2004; received 7 March 2005; revision received 12 September 2005; accepted for publication 16 September 2005. Copyright © 2005 by the American Institute of Aeronautics and Astronautics, Inc. All rights reserved. Copies of this paper may be made for personal or internal use, on condition that the copier pay the \$10.00 per-copy fee to the Copyright Clearance Center, Inc., 222 Rosewood Drive, Danvers, MA 01923; include the code 0731-5090/06 \$10.00 in correspondence with the CCC.

*Assistant Professor, Department of Aeronautical and Space Engineering, corso Duca degli Abruzzi 24. Member AIAA.

†Professor, Department of Mechanics and Aeronautics, via Eudossiana 18. Member AIAA.

‡Graduate Student, Department of Mechanics and Aeronautics, via Eudossiana 18.

nominal behavior of the system is asymptotically recovered when an initial condition that does not lie on \mathcal{S}_0 is considered.

In explicit unfolding, the effects of variations of λ_i are investigated by performing a continuation with respect to μ for each considered value of λ_i , a poorly efficient approach. Moreover, the stability of the solutions on a vertical branch in the augmented phase space $\mathbb{R} \times \mathbb{R}^n$ cannot be investigated during the continuation because all of the solutions remain singular, and their stability can be determined only with some postprocessing of the data obtained from the continuation software. Conversely, the transformation of \mathcal{S}_0 into a globally attractive manifold in the implicit unfolding approach allows the continuation algorithm to determine directly the stability of the limit cycles on \mathcal{S}_0 , a property that is then inferred on the solutions of the nominal system.

Combined use of implicit and explicit unfolding methodologies allows the study of systems where two conserved variables are present, avoiding the computational complexity of continuation in two parameters. The analysis of the simple gyrostat, where both angular momentum \mathbf{h} and kinetic energy \mathcal{T} are conserved, is based on this approach.

When a discrete damper is included in the model, the dynamics of the gyrostat is still confined on the sphere \mathcal{S} of constant $\|\mathbf{h}\|$ due to conservation of angular momentum, even though kinetic energy is not constant.⁹ In this case, implicit unfolding allows one to trace directly branches of periodic solutions induced by rotor unbalance as the relative momentum h_s is varied.

III. Unfolding Branches of Periodic Orbits of Gyrostats

A. Simple Gyrostat Case

As a first test for the determination of periodic solutions of a dual-spin spacecraft by a continuation method, the model of a simple gyrostat with axisymmetric rotor is dealt with. If the pseudoprincipal frame⁵ is used, that is, the principal frame of the pseudoinertia matrix $\mathbf{J} = \mathbf{I} - I_s \hat{\mathbf{a}}\hat{\mathbf{a}}$, where I_s is the rotor moment of inertia about the spin axis $\hat{\mathbf{a}}$, the equations of motion are written in the form⁵

$$\dot{\mathbf{h}} = \mathbf{h} \times \mathbf{J}^{-1}[\mathbf{h} - h_a \hat{\mathbf{a}}], \quad \dot{h}_a = g_a \quad (3)$$

where g_a is the rotor spin torque, $h_a = I_s \omega_s + I_s \omega_s \cdot \hat{\mathbf{a}}$ is the absolute relative angular momentum of the rotor, and ω_s and ω are the rotor speed relative to \mathcal{P} and the platform angular velocity, respectively.

The time derivative of the kinetic energy

$$\mathcal{T} = \frac{1}{2} \omega \cdot \mathbf{I} \omega + h_s \hat{\mathbf{a}} \cdot \omega + \frac{1}{2} (h_s^2 / I_s) \quad (4)$$

is given by $\dot{\mathcal{T}} = \omega_s g_a$. When the apparent gyrostat is dealt with,⁹ g_a is zero, the kinetic energy is constant, and \mathcal{T} is a first integral. If torque-free motions are considered, angular momentum is also conserved, and $M = h^2 = \mathbf{h}^T \mathbf{h}$ is a first integral of Eq. (3) so that the state vector \mathbf{h} evolves on a sphere \mathcal{S} . In what follows, it is assumed that the equations of motion are written in nondimensional form as proposed in Ref. 5, where the components of the angular momentum are scaled with respect to its norm h , and a formally identical expression is obtained such that the vector \mathbf{h}/h is constrained on the unit sphere \mathcal{S}_0 .

To unfold the branch of periodic solutions, the right-hand side of the governing set of equations is augmented by a dissipative term,³ as

$$\dot{\mathbf{h}} = \mathbf{h} \times [\mathbf{J}^{-1} \mathbf{h} - h_a \hat{\mathbf{a}}] + \mu \mathbf{h} \quad (5)$$

When $\mu \mathbf{h}$ is added, the time derivative of \mathcal{T} for the apparent gyrostat becomes $\dot{\mathcal{T}} = \mu \omega \cdot \mathbf{h}$. The equilibria of the system satisfy the relation $\dot{\mathbf{h}} = \mathbf{h} \times \omega = 0$, that is, the angular momentum and platform angular velocity vectors are parallel. This implies that their dot product is nonnull in the equilibrium points, and the additional term $\mu \mathbf{h}$ acts as damping in the neighborhood of the equilibria if its sign is opposite to that of $\omega \cdot \mathbf{h}$. Therefore, μ can be used as the unfolding parameter, and the nominal behavior of the system is recovered when the periodic solutions originating from the Hopf bifurcation in $\mu = 0$ are determined.

Because of conservation of \mathbf{h} , the equilibria of the system for $\mu = 0$ still possess a zero eigenvalue and periodic solutions remain singular because of the presence of a cylinder of solutions parametrized by h . Thus, the introduction of a dissipation term and the use of the unfolding parameter μ are not sufficient for overcoming the problem of Jacobian matrix singularity during the continuation. A suitable approach is to use the implicit unfolding technique, based on augmenting the system dynamics with a term that drives the system toward the unit sphere. For the case of interest, Eq. (3) becomes

$$\dot{\mathbf{h}} = \mathbf{h} \times [\mathbf{J}^{-1} \mathbf{h} - h_a \hat{\mathbf{a}}] + \nu \mathbf{h}(1 - \mathbf{h} \cdot \mathbf{h}) \quad (6)$$

The time derivative of h^2 is

$$\frac{dh^2}{dt} = \frac{d}{dt}(\mathbf{h} \cdot \mathbf{h}) = 2\mathbf{h} \cdot \dot{\mathbf{h}} = 2\nu h^2(1 - h^2)$$

so that, for $\nu > 0$, the additional term in Eq. (6) acts as a torque in the direction of \mathbf{h} when its modulus is smaller than unity, whereas it is in the direction opposite to \mathbf{h} otherwise. The additional term is zero only when \mathbf{h} lies on \mathcal{S}_0 , and the nominal behavior of the system is recovered, or in the trivial case $\mathbf{h} = 0$. It can be easily demonstrated that the latter equilibrium is unstable for the dynamic system represented by Eq. (6), and, therefore, outside the origin the unit sphere is globally attractive for the augmented system. Periodic solutions of Eq. (6) exist only on \mathcal{S}_0 , where they also are solutions for the nominal system described by Eq. (3).

In conclusion, the governing equation of the gyrostat is augmented by $\mu \mathbf{h} + \nu \mathbf{h}(1 - \mathbf{h} \cdot \mathbf{h})$, where the first term contains the explicit unfolding parameter and the second term eliminates the singularity due to the conservation of angular momentum, attracting all of the solutions on the unit sphere and destroying the cylinder of solutions parametrized by h . In Figs. 1a–1c periodic solutions for the set of gyrostat parameters used in Ref. 5 are shown for values of h_a equal to 0.16, 0.25, and 1.0 (despun platform), respectively. The orbits are regularly spaced over the unit sphere and the continuation is only interrupted when an etheroclinic or homoclinic orbit (dashed lines in Figs. 1a and 1b) is approached.

Note that the additional term that transforms the unit sphere \mathcal{S}_0 into a globally attractive subset of the phase space does not require that this manifold is a sphere, which means that implicit unfolding may be applied even for first integrals different from the norm of a vector quantity. Nonetheless, when $M = \text{const}$ over a more complex manifold, demonstration of global attractiveness may become difficult to prove.

B. Gyrostat with Discrete Damper and Unbalanced Rotor

The equations of motion of the gyrostat with a discrete damper reported in Ref. 9 can be written in nondimensional form

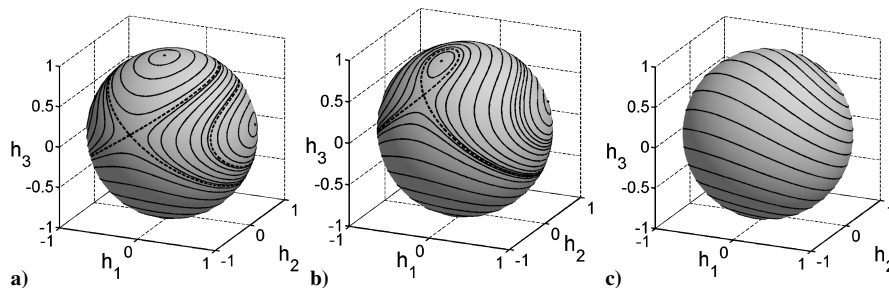


Fig. 1 Case 1: periodic solutions for a) $h_a = 0.16$, b) $h_a = 0.32$, and c) $h_a = 1.0$.

as⁶

$$\dot{\mathbf{h}} = \mathbf{h} \times \mathbf{K}^{-1} \mathbf{m}$$

$$\dot{p}_n = -(m_d/m) \mathbf{m} \cdot \mathbf{K}^{-1} \hat{\mathbf{n}} \times \{ [\mathbf{b} + (1 - m_d/m) \delta \hat{\mathbf{n}}] \times \mathbf{K}^{-1} \mathbf{m} \} - c_d v - k \delta$$

$$\dot{\delta} = v, \quad \dot{h}_a = g_a \quad (7)$$

where the states are the components of the nondimensional angular momentum $\mathbf{h} = (h_1, h_2, h_3)^T$, written in a body frame \mathcal{F}_B fixed with respect to the satellite platform \mathcal{P} ; the momentum component p_n of the damper mass m_d in the direction $\hat{\mathbf{n}}$ of the damper, the position δ of the mass along the damper (the position vector \mathbf{b} indicating the rest position of m_d), and the axial component h_a of the absolute angular momentum stored in the rotor (where g_a is the torque applied to the rotor spin axis). The inertia matrix in Eq. (7) is given by

$$\mathbf{K} = \mathbf{I}_0 + (m_d/m) [2\delta \mathbf{b} \cdot \hat{\mathbf{n}} \mathbf{1} - \delta (\mathbf{b} \hat{\mathbf{n}} + \hat{\mathbf{n}} \mathbf{b}) + (1 - m_d/m) \delta^2 (\mathbf{1} - \hat{\mathbf{n}} \hat{\mathbf{n}})] \quad (8)$$

where $\mathbf{1}$ is the 3×3 identity matrix, whereas the vector \mathbf{m} in Eq. (7) is

$$\mathbf{m} = \mathbf{h} - h_s \hat{\mathbf{a}} - v(m_d/m) \mathbf{b} \times \hat{\mathbf{n}} \quad (9)$$

with the usual meaning of the symbols.⁶ The relative velocity v of the mass m_d in the damper is

$$v = \left(\frac{m}{m_d} \right) \frac{p_n + (m_d/m) \hat{\mathbf{n}} \cdot \mathbf{b} \times \mathbf{K}^{-1} (\mathbf{h} - I_s \omega_s \hat{\mathbf{a}})}{1 - (m_d/m) + (m_d/m) \hat{\mathbf{n}} \cdot \mathbf{b} \times \mathbf{K}^{-1} (\mathbf{b} \times \hat{\mathbf{n}})}$$

When a dynamically unbalanced rotor is dealt with, a parameter ε is introduced such that the perturbed rotor transverse inertia is given by $I_t = (1 + \varepsilon) I_{t0}$, the unit vector of the perturbed principal axis being $\hat{\mathbf{t}}$. In this case, the pseudoinertia matrix becomes

$$\mathbf{K} = \mathbf{I}_0 + (m_d/m) [2\delta \mathbf{b} \cdot \hat{\mathbf{n}} \mathbf{1} - \delta (\mathbf{b} \hat{\mathbf{n}} + \hat{\mathbf{n}} \mathbf{b}) + (1 - m_d/m) \delta^2 \times (\mathbf{1} - \hat{\mathbf{n}} \hat{\mathbf{n}})] + \varepsilon I_t \hat{\mathbf{t}} \hat{\mathbf{t}} \quad (10)$$

and a forcing term appears because of the change of mass distribution induced by the rotor spinning at a relative angular velocity ω_s . Given a constant relative rotor angular speed, as for the Kelvin gyrost (see Ref. 9), the angular position of the rotor can be expressed in terms of the components of $\hat{\mathbf{t}}$

$$\hat{\mathbf{t}} = \omega_s \hat{\mathbf{a}} \times \hat{\mathbf{t}} \quad (11)$$

Finally, the equation for the absolute component h_a of the rotor spin angular momentum becomes

$$\dot{h}_a = g_a + \varepsilon I_t \omega_s \cdot (\hat{\mathbf{a}} \times \hat{\mathbf{t}}) (\hat{\mathbf{t}} \cdot \omega) \quad (12)$$

where the term $\varepsilon I_t \omega$ is the result of rotor unbalance. Note that, when a constant relative angular momentum component h_s is considered, Eq. (12) is not included in the model, and it is assumed that a proper control action on the rotor spin torque g_a is devised to keep the rotor at a constant relative angular velocity ω_s . In all of the considered cases, the principal frame of the spacecraft for $\delta = 0$ and $\varepsilon = 0$ is used as the reference frame \mathcal{F}_B .

To study the closed orbits of periodically forced nonautonomous systems using continuation algorithms, it is common practice¹⁰ to express the forcing term $F = F_{\max} \sin(\Omega t)$ as $F = F_{\max} f$, where f is the first state variable of the nonlinear system

$$\dot{f} = \Omega g + f(1 - f^2 - g^2), \quad \dot{g} = -\Omega f + g(1 - f^2 - g^2)$$

the solution of which asymptotically converges onto the limit cycle $f = \sin(\Omega t)$, $g = \cos(\Omega t)$. The resulting autonomous system has a phase space augmented of two dimensions with respect to the original problem (dimension n). This is detrimental to the numerical efficiency of the continuation algorithm because of the significant increase in the order of the equivalent algebraic set of equations, due to the higher number of intervals and/or Gauss collocation points necessary for the discretization of the periodic solutions, multiplied

by the (increased) dimension of the phase space.¹⁰ A novel technique for including a periodic forcing term is adopted here, based on the definition of two auxiliary coordinates

$$X = (x_i + K) \sin(\Omega t) = (x_i + K) \sin(\tau)$$

$$Y = (x_i + K) \cos(\Omega t) = (x_i + K) \cos(\tau)$$

the evolution of which is ruled by the state equations

$$\begin{aligned} \dot{X} &= \dot{x}_i \sin(\tau) + \Omega (x_i + K) \cos(\tau) \\ \dot{Y} &= \dot{x}_i \cos(\tau) - \Omega (x_i + K) \sin(\tau) \end{aligned} \quad (13)$$

where x_i is a state variables bounded in modulus by K , that is, $|x_i(t)| < K$, and $\tau = \text{mod}(\Omega t, 2\pi)$. The i th equation of the vector field \dot{x}_i is replaced by Eqs. (13) to obtain an equivalent dynamic system where $x_i = [X^2 + Y^2]^{1/2} - K$ and $\tau = \tan^{-1}(Y/X)$. In this way, the dimension of the phase space of the equivalent autonomous system is limited to $n + 1$.

With the augmented system, the analysis of steady-state limit cycles of a gyrost with an unbalanced rotor is performed for different values of $h_s = I_s \omega_s$. The branch of stable limit cycles thus obtained indicates the route followed by the gyrost state variables during a platform despin maneuver, with a small spin torque g_a . The nominal configuration is the same of Ref. 6 and is reported in Table 1, where the rotor transverse inertia is $I_t = 0.02$, as for a flat momentum wheel.

Figure 2a shows the limit cycles on \mathcal{S}_0 of a gyrost with an unbalanced rotor ($\varepsilon = 0.25$), for values of h_s between 0 and 1, where $h = 0$ corresponds to an all-spun condition, that is, the rotor is fixed with respect to the platform, and $h = 1$ is for a completely despun platform. Limit cycles traced in black are stable whereas white lines show unstable solutions.

The limit cycle structure resembles very closely the sequence of equilibria determined by Sandfry and Hall⁶ for the axial rotor case, inasmuch as the amplitude of the limit cycles is negligible for $0.1 < h_s < 1$, in spite of rotor unbalance. Therefore, when the frequency of the forcing term induced by not perfectly equal rotor transverse inertias is sufficiently high, the response of the platform is negligible, thus demonstrating that the effect of dynamic rotor unbalance on final attitude is slight for the proposed set of gyrost parameters.

Table 1 Gyrost data for the nominal case⁶

Parameter	Symbol	Value
<i>Satellite</i>		
Inertia tensor (nominal case)	\mathbf{I}_0	diag(0.28, 0.32, 0.4)
<i>Rotor</i>		
Spin axis inertia parameter	I_s	0.04
Spin axis	\mathbf{a}	$(0, 0, 1)^T$
<i>Damper</i>		
Mass parameter	m_d/m	0.1
Damper orientation	\mathbf{n}	$(0, 0, 1)^T$
Rest position	\mathbf{b}	$(0, 0, 0.5)^T$
Spring stiffness	k	0.4
Damping coefficient	c	0.1

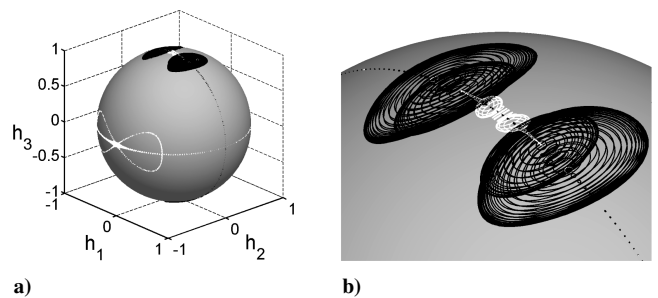


Fig. 2 Case 2: limit cycles for $0 < h_s < 1$.

Limit cycle amplitude, not negligible for $h_s < 0.1$, becomes sizable for $h_s < 0.02$ as is apparent in the enlargement shown in Fig. 2b. Actually, these limit cycles exist for a narrow range of values of h_s , and they do not influence significantly the first part of the spin-up maneuver if the spin-up torque is sufficiently high, provided that large oscillations are not allowed to build up by rapidly increasing h_s beyond 0.02.

Other situations were addressed by varying the damper mass parameter or analyzing the effect of a nutation damper. In the first case, not shown in the figures, the structure of the periodic solutions is completely changed even though the existence of large-amplitude stable limit cycles is again confined to low values of h_s . When a nutation damper is used, such that $\mathbf{n} = (0, 1, 0)^T$, the despin maneuver follows one of the two stable branches shown in Fig. 3a, whereas the branch of solutions symmetric with respect to h_2 becomes unstable. For each value of h_s there are two stable limit cycles characterized by values of h_2 of opposite sign and a phase shift of 180 deg in the damper mass position during the oscillation.

An interesting situation is apparent when a misalignment between rotor spin axis and a precession damper is considered. For a damper inclined in the x - y plane by 10 deg with respect to the original orientation [$\mathbf{n} = (0.985, 0.174, 0)^T$], the structure of the solutions remains similar to that obtained for $\mathbf{n} = \mathbf{a} = (1, 0, 0)^T$, but for low values of h_s . In that region, shown in Fig. 3b, two folds are found on S_0 with a branch of unstable limit cycles connecting two anti-symmetric branches of stable solutions that again show the paths followed by the gyrostat during a despin at low g_a .

This apparently marginal modification in a region of the phase space that proved to be of some interest only during the initial phases

of the platform despin in the previous cases has, on the converse, considerable consequences on the maneuver that become much more sensitive to the initial all-spun condition. If the platform manages to follow the branch of stable solutions, the despin is smooth and similar to that performed in the nominal case, in spite of the damper misalignment. However, large oscillations build up when the fold is crossed.

The time history of the angular momentum components during rotor spin-up for $g_a = 0.001$, represented by the dashed line on S_0 in Fig. 3b, shows that the trajectory jumps to a different stable branch because of the fold at $h_s = 0.13$. The phenomenon is also clearly visible in the bifurcation diagrams of Fig. 4a–4c, where the amplitude of periodic orbits are traced as a function of h_s . Large oscillations are experienced during the whole maneuver, the amplitude of which decreases slowly as h_s increases.

IV. Conclusions

Analysis of periodic orbits for conservative system was carried out in the framework of numerical continuation by the novel method of implicit unfolding.

Application to the simple gyrostat, where implicit unfolding was adopted in conjunction with explicit unfolding for dealing with periodic orbit singularity due to the presence of two conserved variables, shows that the entire phase portrait of the system can be efficiently determined for different values of the absolute angular momentum stored in the rotor.

The analysis of the gyrostat with damper and dynamically unbalanced rotor was then performed to investigate the effects of a periodic forcing term on the structure of stable and unstable closed orbits when the rotor relative angular speed is varied, as in a platform despin maneuver. Different sets of system parameters were considered to unveil critical situations, such as the buildup of large-amplitude oscillations during despin when the damper is not perfectly aligned with the rotor spin axis.

References

- ¹Doedel, E. J., Keller, H. B., and Kernevez, J. P., "Numerical Analysis and Control of Bifurcation Problems: (i) Bifurcation in Finite Dimensions," *International Journal of Bifurcation and Chaos*, Vol. 1, No. 3, 1991, pp. 493–520.
- ²Doedel, E. J., Keller, H. B., and Kernevez, J. P., "Numerical Analysis and Control of Bifurcation Problems: (ii) Bifurcation in Infinite Dimensions," *International Journal of Bifurcation and Chaos*, Vol. 1, No. 4, 1991, pp. 745–772.

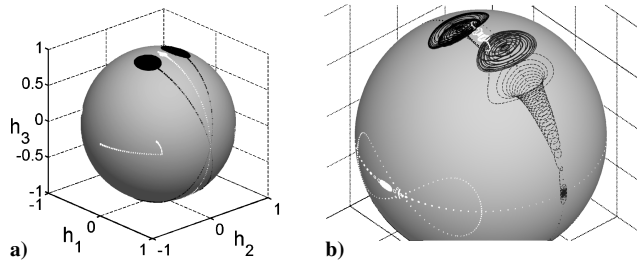


Fig. 3 Case 2: gyrostat equipped with a) a nutation damper and b) a misaligned axial damper.

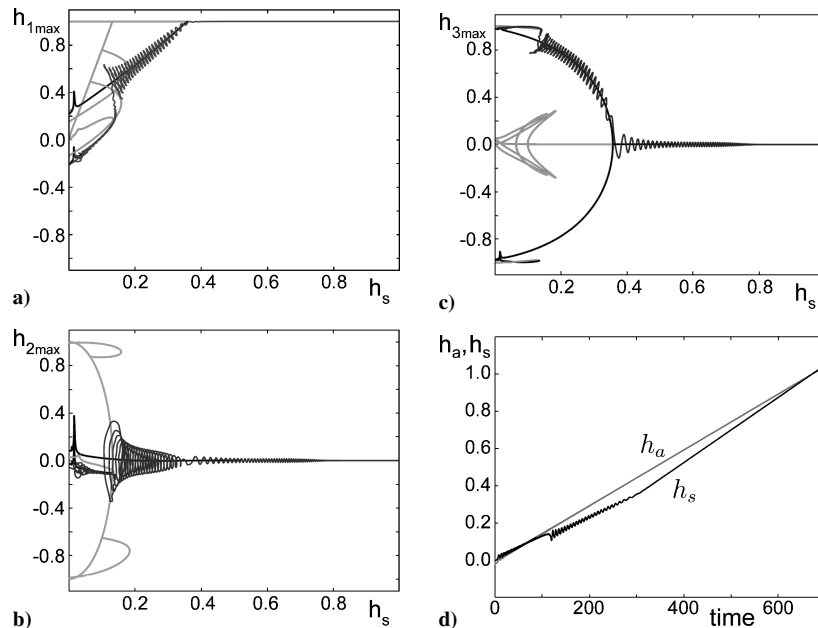


Fig. 4 Bifurcation diagrams for a)–c) the misaligned damper case and d) the evolution of h_s and h_a .

³Muñoz-Almaraz, F. J., Freire, E., Galn, J., Doedel, E., and Vanderbauwhede, A., "Continuation of Periodic Orbits in Conservative and Hamiltonian Systems," *Physica D: Nonlinear Phenomena*, Vol. 181, No. 1, 2003, pp. 1–38.

⁴Paffenroth, R. C., Doedel, E. J., and Dichmann, D. J., "Continuation of Periodic Orbits Around Lagrange Points and AUTO2000," American Astronautical Society Paper AAS 01-303, Aug. 2001.

⁵Hall, C. D., "Spinup Dynamics of Gyrostats," *Journal of Guidance, Control, and Dynamics*, Vol. 18, No. 5, 1995, pp. 1177–1183.

⁶Sandfry, R. A., and Hall, C. D., "Relative Equilibria of a Gyrostat with a Discrete Damper," *Journal of the Astronautical Sciences*, Vol. 50, No. 4, 2003, pp. 367–387.

⁷Sandfry, R. A., and Hall, C. D., "Steady Spins and Spinup Dynamics of Nearly Axisymmetric Dual-Spin Satellites with Damping," *Journal of Spacecraft and Rockets*, Vol. 41, No. 6, 2004, pp. 948–955.

⁸Meyer, K. R., *Introduction to Hamiltonian Dynamical Systems and the N-Body Problem*, Springer-Verlag, New York, 1992, pp. 129–136.

⁹Hughes, P. C., *Spacecraft Attitude Dynamics*, Wiley, New York, 1986, pp. 156–225.

¹⁰Doedel, E. J., Paffenroth, R. C., Champneys, A. R., Fairgrieve, T. F., Kuznetsov, Yu. A., Sandstede, B., and Wang, X., "AUTO 2000: Continuation and Bifurcation Software for Ordinary Differential Equations (with Hom-Cont)," Technical Rept., California Inst. of Technology, Pasadena, CA, Feb. 2001, URL: <http://sourceforge.net/projects/auto2000/> [cited 28 June 2002].